

FREE VIBRATIONS IN A PERIODICALLY RIBBED ELASTIC PLATE

Katarzyna Jeleniewicz, Wiesław Nagórko

Warsaw University of Life Sciences – SGGW

Abstract. In the paper we consider plates reinforced by ribs. Assuming a periodic distribution of the ribs in the plate, an averaged model is being constructed. The method used here is not asymptotic. In the modelling equations a microstructure parameter remains (basic cell size). To test out the model, a case of free vibrations is being analyzed.

Key words: ribbed plate, elastodynamics of plates, methods of homogenization, vibrations of plates

INTRODUCTORY CONCEPTS

The paper deals rectangular elastic plates reinforced by periodically spaced ribs (Fig. 1). It is assumed that the plate is subjected to the plane stress. In the reference configuration the plate occupy the region $\Pi = (-L, L) \times (-H, H)$, $(x_1, x_2) \in \Pi$. The limit passage $L \rightarrow \infty$ leads to the plate-band. By I we denote a known time interval, $t \in I \subset R$. The plate will be reinforced by the ribs of thickness l' and l'' , respectively spaced and parallel to x_2 -axis. Distances between the ribs are equal.

The basic cell coincide with the $\Delta = (-l, l)$. Hence the length of this cell is equal to $2l$. In this case the distances between the ribs are equal $l - \frac{l' + l''}{2}$. It will be assumed that $l' + l'' \ll 2l$.

The plate material is homogeneous and isotropic with Lamé module λ , μ and mass density M_0 . Under the plate stress assumption modulus λ will be replaced by the reduced

$$\text{modulus } \lambda_0 \equiv \frac{2\lambda\mu}{1+2\mu}.$$

Corresponding author – Adres do korespondencji: Katarzyna Jeleniewicz, Szkoła Główna Gospodarstwa Wiejskiego, Katedra Budownictwa i Geodezji, ul. Nowoursynowska 159, 02-776 Warszawa, e-mail: k.jeleniewicz@tlen.pl

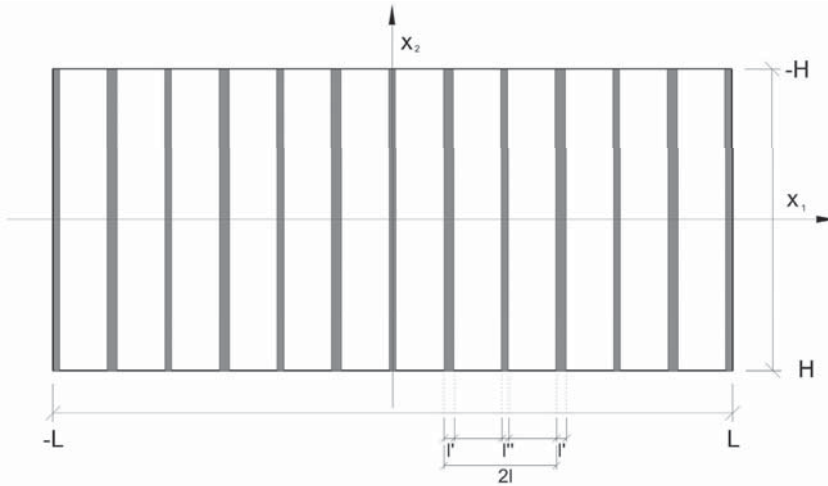


Fig. 1. Rectangular elastic plates reinforced by periodically spaced ribs

Rys. 1. Prostokątna sprężysta płyta zbrojona periodycznie rozmieszczonymi żebrami

The ribs are assumed to be slender in Ox_1x_2 – plate and carried out only axial stresses. Hence their mechanical (materials) properties are determined by Young modulus (E_α) and mass density (M_α), $\alpha = 1, 2$. Moreover, the thickness of ribs will be neglected as small when compared to the distance (l) between the ribs axes. At the same time we shall assume that l is very small with respect to characteristic length dimension of Ω , L , $l \ll L$ as shown in Figure 1.

We denote by $w_\alpha(x_1, x_2, t)$, $\alpha = 1, 2$, $x_1 \in (-L, L)$, $x_2 \in (-H, H)$, $t \in R$ components of the displacement vector field in Ox_1x_2 – plane (the total plate deflection). In the subsequent consideration, summation convention with respect to subscripts α, β, \dots holds. The boundary conditions for the plate are assumed in the form:

$$w_1(\pm L, x_2, t) = 0, \quad w_2(x_1, \pm H, t) = 0, \quad (\partial_2 w_1 + \partial_1 w_2)(x_1, \pm H, t) = 0 \quad (1)$$

For the plate-band boundary conditions on $x_1 = \pm L$ will be ignored.

Introducing Dirac functions $\delta(\cdot)$ of argument $x_1 \in R$ and setting [Nagórko and Woźniak 2002]:

$$\tilde{M}_\alpha(x_1) = M_\alpha \delta(x_1 \pm l_\alpha)$$

$$\tilde{E}_\alpha(x_1) = E_\alpha \delta(x_1 \pm l_\alpha), \quad \alpha = 1, 2, \dots$$

where $l_1 = (2n - l)l$, $l_2 = 2nl$, $n = 0, \pm 1, \pm 2, \dots$, we can define

$$\rho(x_1) = M_0 + \tilde{M}_1(x_1) + \tilde{M}_2(x_1)$$

$$C_{\alpha\beta\gamma\delta}(x_1) = \lambda_0 \delta_{\alpha\beta} \delta_{\gamma\delta} + \mu (\delta_{\alpha\gamma} \delta_{\beta\delta} + \delta_{\alpha\delta} \delta_{\beta\gamma}) + (\tilde{E}_1 + \tilde{E}_2) \delta_{\alpha 2} \delta_{\beta 2} \delta_{\gamma 2} \delta_{\delta 2}$$

The aim of this papers is to applied the tolerance modelling method [Woźniak and Wierzbicki 2000], to analysis of free vibrations of the plate.

MODELLING PROCEDURE

The modeling procedure begins with the well known form of Lagrangian for the plane stress problem under consideration

$$L = \frac{1}{2} \rho \dot{w}_\alpha \dot{w}_\alpha - \frac{1}{2} C_{\alpha\beta\gamma\delta} w_{\alpha,\beta} w_{\gamma,\delta} \quad (2)$$

and the system of equations

$$\rho(x_1) \ddot{w}_\alpha(x_1, x_2, t) - [C_{\alpha\beta\gamma\delta}(x_1) w_{\gamma,\delta}]_{,\beta} = 0 \quad (3)$$

for the total plate deflection $w_\alpha(\cdot)$, which has highly oscillating coefficients.

According to the tolerance averaging technique we assume the decomposition of displacement fields in a form

$$w_\alpha(x_1, x_2, t) = u_\alpha(x_1, x_2, t) + h(x_1)v_\alpha(x_1, x_2, t) \quad (4)$$

where $u_\alpha(\cdot, x_2, t)$ and $v_\alpha(\cdot, x_2, t)$ are slowly-varying functions and the function $h(x_1)$ are known $2l$ -periodic, fluctuations shape functions, in the form given in Figure 2. It will be assumed that $a = 1$.

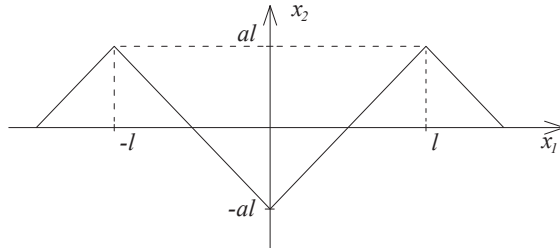


Fig. 2. Fluctuation shape function $h(\cdot)$

Rys. 2. Funkcja kształtu $h(\cdot)$

Substitute the displacement fields (4) to the functional (2) and averaging this functional [Thermomechanics of mikroheterogeneous... 2008], we obtain:

$$\begin{aligned} < L > = & \frac{1}{2} [< \rho > \dot{u}_\alpha \dot{u}_\alpha + < \rho h^2 > \dot{v}_\alpha \dot{v}_\alpha + < C_{\alpha\beta\gamma\delta} > u_{\alpha,\beta} u_{\gamma,\delta} + 2 < C_{\alpha\beta\gamma\delta} h' > u_{\alpha,\beta} v_\gamma + \\ & + < C_{\alpha\beta\gamma\delta} h^2 > v_{\alpha,\beta} v_{\gamma,\delta} + < C_{\alpha\beta\gamma\delta} (h')^2 > v_\alpha v_\beta] \end{aligned}$$

where $h' = \partial h / \partial x_1$ and the averaging operator, for every integrable functions f is defined as:

$$< f > = \frac{1}{2l} \int_{-l}^l f(x_1) dx_1$$

Applying Euler-Lagrange equations we arrive at the system of the tolerance model equations:

$$\begin{aligned} & \langle \rho \rangle \ddot{u}_\alpha - \langle C_{\alpha\beta\gamma\delta} \rangle u_{\gamma,\beta\delta} + \langle C_{\alpha\beta\gamma l} h' \rangle v_{\gamma,\beta} = 0 \\ & \langle \rho h^2 \rangle \ddot{v}_\alpha - \langle C_{\alpha 2\beta 2} h^2 \rangle v_{\beta,22} + \langle C_{\alpha l \beta \gamma} h' \rangle u_{\beta,\gamma} + \langle C_{\alpha l \beta l} (h')^2 \rangle v_\beta = 0 \end{aligned} \quad (5)$$

It can be seen that the above modelling approach leads from equations (3) to the system of equations (5) for the averaged deflection $u_\alpha(\cdot)$ and fluctuation variable $v_\alpha(\cdot)$, $\alpha = 1, 2$. Equations (5) have constant coefficients and hence constitute the proper mathematical tool for the analysis of special problems. It has to be emphasized that solutions to the boundary-value problems for the above equations have a physical sense only if $u_\alpha(\cdot, x_2, t)$, $v_\alpha(\cdot, x_2, t)$ are slowly varying functions:

$$u_\alpha(\cdot, x_2, t) \in S_\delta^1 V(\Delta), \quad v_\alpha(\cdot, x_2, t) \in SV_\delta^1(\Delta) \quad (6)$$

for every $x_2 \in (-H, H)$ and every time .

Summarizing the obtained results we can state that the derived non-asymptotic model of a ribbed plate under considerations is governed by the system of equations (5) for the basic unknowns $u_\alpha(\cdot)$ and $v_\alpha(\cdot)$, by the physical reliability conditions (6) and by the approximation formula (4) for total plate deflections. It can be observed that the constant coefficients in (4), which depend on $h(x_1)$, describe the effect of the microstructure size l on the averaged behavior of the ribbed plate.

ANALYSIS

It will be shown that the analysis of the problem under consideration can be carried out under some additional assumptions:

$$\begin{aligned} u_1 &= u_1(x_1, t), \quad v_1 = v_1(x_1, t), \quad x_1 \in [-L, L] \\ u_2 &= u_2(x_2, t), \quad v_2 = v_2(x_2, t), \quad x_2 \in [-H, H] \end{aligned} \quad (7)$$

Taking into account the terms (7) in the equations (4), we obtain:

$$\begin{aligned} & \langle \rho \rangle \ddot{u}_1 - \langle C_{1111} \rangle u_{1,11} + \langle C_{1111} h' \rangle v_{1,1} + \langle C_{1212} h' \rangle v_{2,2} = 0 \\ & \langle \rho h^2 \rangle \ddot{v}_1 - \langle C_{1111} h' \rangle u_{1,1} + \langle C_{1122} h' \rangle u_{2,2} + \langle C_{1111} (h')^2 \rangle v_1 = 0 \\ & \langle \rho \rangle \ddot{u}_2 - \langle C_{2222} \rangle u_{2,22} = 0 \\ & \langle \rho h^2 \rangle \ddot{v}_2 - \langle C_{2222} h^2 \rangle v_{2,22} + \langle C_{1212} (h')^2 \rangle v_2 = 0 \end{aligned} \quad (8)$$

The function, which is shown in Figure 2, has the following form:

$$h(x_1) = \begin{cases} -2x_1 - l & x_1 \in [-l, 0] \\ 2x_1 - l & x_1 \in [0, l] \end{cases} \quad (9)$$

Hence, the coefficients in the equations (8), are equal to:

$$\begin{aligned}
 <\rho> &= < M_0 + \tilde{M}_1 + \tilde{M}_2 > = M_0 + \frac{M_1 + M_2}{2l} \\
 < C_{1111} > &= < \lambda_0 + 2\mu > = \lambda_0 + 2\mu \\
 < C_{2222} > &= < \lambda_0 + 2\mu + \tilde{E}_1 + \tilde{E}_2 > = \lambda_0 + 2\mu + \frac{E_1 + E_2}{2l} \\
 < \rho h^2 > &= < (M_0 + \tilde{M}_1 + \tilde{M}_2) h^2 > = l^2 \left(\frac{M_0}{3} + \frac{(M_1 + M_2)}{2l} \right) \\
 < C_{2222} h^2 > &= < (\lambda_0 + 2\mu + \tilde{E}_1 + \tilde{E}_2) h^2 > = l^2 \left(\frac{(\lambda_0 + 2\mu)}{3} + \frac{(E_1 + E_2)}{2l} \right) \\
 < C_{1111} h' > &= < (\lambda_0 + 2\mu) h' > = 0 \\
 < C_{1212} h' > &= < \mu h' > = 0 \\
 < C_{1122} h' > &= < \lambda_0 h' > = 0 \\
 < C_{1111} (h')^2 > &= < (\lambda_0 + 2\mu) (h')^2 > = 4(\lambda_0 + 2\mu) \\
 < C_{1212} (h')^2 > &= < \mu (h')^2 > = 4\mu
 \end{aligned} \tag{10}$$

Substituting the coefficients (10) into equations (8) we arrive at the system of the tolerance model equations. This system consists of two independent equations for $u_1(x_1, t)$ and $v_1(x_1, t)$, in which $x_1 \in [-L, L]$:

$$\begin{aligned}
 \left(M_0 + \frac{M_1 + M_2}{2l} \right) \ddot{u}_1 - (\lambda_0 + 2\mu) u_{1,11} &= 0 \\
 l^2 \left(\frac{M_0}{3} + \frac{M_1 + M_2}{2l} \right) \ddot{v}_1 + 4(\lambda_0 + 2\mu) v_1 &= 0
 \end{aligned} \tag{11}$$

and two independent equations for $u_2(x_3, t)$ $v_2(x_2, t)$, in which $x_2 \in [-H, H]$:

$$\begin{aligned}
 \left(M_0 + \frac{M_1 + M_2}{2l} \right) \ddot{u}_2 - \left(\lambda_0 + 2\mu + \frac{E_1 + E_2}{2l} \right) u_{2,22} &= 0 \\
 l^2 \left(\frac{M_0}{3} + \frac{M_1 + M_2}{2l} \right) \ddot{v}_2 - l^2 \left(\frac{\lambda_0 + 2\mu}{3} + \frac{E_1 + E_2}{2l} \right) v_{2,22} + 4\mu v_2 &= 0
 \end{aligned} \tag{12}$$

It has to be emphasized that these equations makes it admit boundary conditions (1) for arbitrary positive H, L . Hence:

$$u_1(\pm L, t) = 0, v_1(\pm L, t) = 0, \quad u_2(\pm H, t) = 0, v_2(\pm H, t) = 0 \tag{13}$$

Now let us pass to analysis of the equations (12). This equation can be rewritten in the form:

$$\ddot{v}_2 - A_2 v_{2,22} + B_2 v_2 = 0$$

where

$$A_2 = \frac{2l(\lambda_0 + 2\mu) + 3(E_1 + E_2)}{2lM_0 + 3(M_1 + M_2)}, \quad B_2 = \frac{24\mu}{(2lM_0 + 3(M_1 + M_2))l}$$

Setting $v_2(x_2, t) = \psi(x_2)\xi(t)$ (where $\xi(t) = \cos \omega t$) we obtain:

$$A\psi'' - (B - \omega^2)\psi = 0 \quad (14)$$

We shall consider the following special cases:

- if $B > \omega^2$, then $\psi'' - \kappa^2\psi = 0$, where $\kappa^2 = \frac{B - \omega^2}{A}$, hence $\psi = C_1 e^{-\kappa x_2} + C_2 e^{\kappa x_2}$, including the condition (13)₄ we obtain $C_1 = C_2 = 0$,
- if $B < \omega^2$, then denoting $\kappa^2 = \frac{\omega^2 - B}{A}$ we obtain $\psi'' + \kappa^2\psi = 0$, it follows that $\psi = C_1 \cos \kappa x_2 + C_2 \sin \kappa x_2$.

Taking into account the solution of (14) in form $\psi = C_1 \cos \kappa x_2$, we obtain $\kappa = \kappa_n = \frac{\pi}{2H} + \frac{n\pi}{H}$, $n = 0, \pm 1, \pm 2$, and $\omega_n = -A_2 \kappa_n^2 + B_2$. Finally:

$$v_2(x_2, t) = C_n \cos \kappa_n x_2 \cos \omega_n t \quad (15)$$

Under denotation $A_l = \frac{2l(\lambda_0 + 2\mu) + (E_1 + E_2)}{2lM_0 + M_1 + M_2}$, the equation (12)₁ takes form

$\ddot{u}_2 - A_l u_{2,22} = 0$. Introducing solutions in the similar form as before $u_2(x_2, t) = \psi(x_2) \cos \omega t$ we obtain:

$$\psi = C_1 \cos \kappa x_2 + C_2 \sin \kappa x_2 \text{ where } \kappa^2 = \tilde{\omega}^2 / A_l$$

Assuming $C_2 = 0$, from condition (13)₃, we can determine the free vibrations $\tilde{\omega}_n^2 = A_l \kappa_n^2$, $n = 0, \pm 1, \pm 2, \dots$ Finally we obtain:

$$u_2(x_2, t) = C_n \cos \kappa_n x_2 \cos \tilde{\omega}_n t \quad (16)$$

Taking into account conditions (13)₁₋₂, we arrive at the solutions of the equations (11) in the form:

$$\begin{aligned} u_l(x_l, t) &= C_n \cos \bar{\kappa}_n x_l \cos \bar{\omega}_n t \\ v_l(x_l, t) &= C_n (x_l^2 - L^2) \cos \sqrt{B_0} t \end{aligned} \quad (17)$$

where $\bar{\kappa}_n^2 = \bar{\omega}_n^2 / A_l$, $\bar{\omega}_n = A_0 \left(\frac{\pi}{2L} + \frac{n\pi}{L} \right)$, $n = 0, \pm 1, \pm 2, \dots$

$$A_0 = \frac{2l(\lambda_0 + 2\mu)}{2lM_0 + M_1 + M_2}, \quad B_0 = \frac{12(\lambda_0 + 2\mu)}{2lM_0 + 3(M_1 + M_2)}$$

To plot graphs of the analytical solutions (15) – (17) we shall assume following values of the material constants of the plate and the ribs: $\mu^M = 11,25 \text{ GPa}$, $\lambda^M = 7,5 \text{ GPa}$, $E^R = E_1 = E_2 = 200 \text{ GPa}$, the plate mass density and the ribs mass density will be equal to: $M^M = M_0 = 2400 \text{ kg} \cdot \text{m}^{-3}$, $M^R = M_1 = M_2 = 7900 \text{ kg} \cdot \text{m}^{-3}$, respectively. The dimensions of the plate will be equal to $L = 5 \text{ m}$, $H = 5 \text{ m}$, $l = 0,3 \text{ m}$.

Figure 3 shows the graph of the averaged displacement $u_1 = u_1(x_1, t)$ related to the first free frequency. The graph of function $u_2 = u_2(x_2, t)$ is similar.

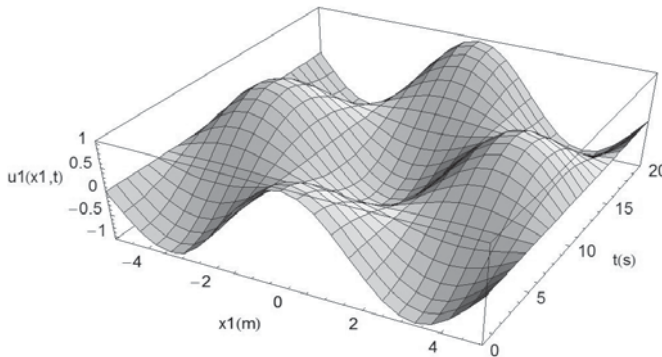


Fig. 3. Graph of $u_1 = u_1(x_1, t)$, at $n = 1$

Rys. 3. Wykres $u_1 = u_1(x_1, t)$ dla $n = 1$

Cross-sections through the graphs of the averaged displacements u_1 , u_2 for various times $t = 5, 10, 15 \text{ s}$ are shown on the graphs 4, 5, 6.

Graphs of fluctuations $v_1 = v_1(x_1, t)$, $v_2 = v_2(x_2, t)$ are illustrate on Figures 7, 8.

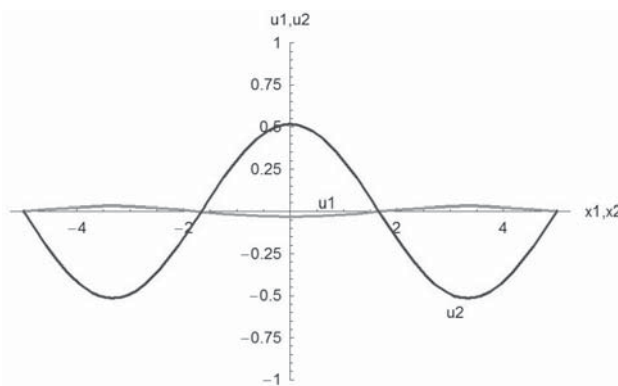


Fig. 4. Cross-section through the graphs $u_1 = u_1(x_1, t)$, $u_2 = u_2(x_2, t)$ for the fixed time $t = 5 \text{ s}$

Rys. 4. Przekrój przez wykresy $u_1 = u_1(x_1, t)$, $u_2 = u_2(x_2, t)$ dla ustalonego czasu $t = 5 \text{ s}$

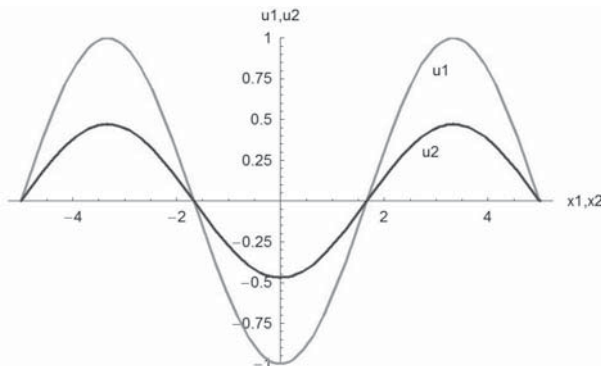


Fig. 5. Cross-section through the graphs $u_1 = u_1(x_1, t)$, $u_2 = u_2(x_2, t)$ for the fixed time $t = 10$ s
Rys. 5. Przekrój przez wykresy $u_1 = u_1(x_1, t)$, $u_2 = u_2(x_2, t)$ dla ustalonego czasu $t = 10$ s

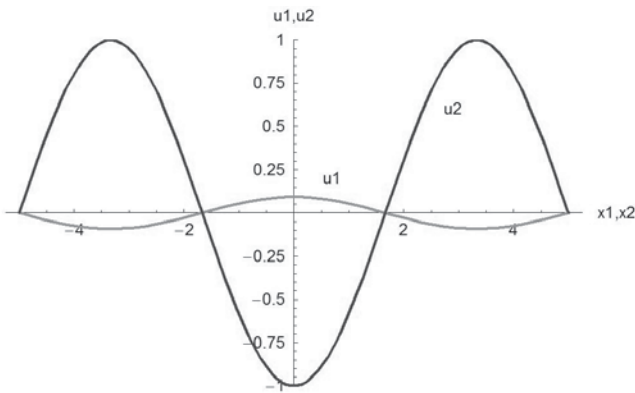


Fig. 6. Cross-section through the graphs $u_1 = u_1(x_1, t)$, $u_2 = u_2(x_2, t)$ for the fixed time $t = 15$ s
Rys. 6. Przekrój przez wykresy $u_1 = u_1(x_1, t)$, $u_2 = u_2(x_2, t)$ dla ustalonego czasu $t = 15$ s

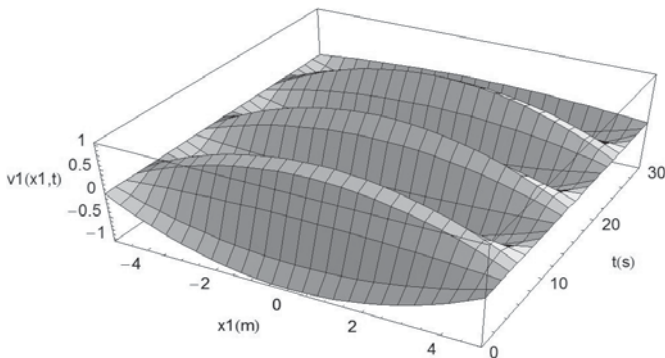


Fig. 7. Graph of $v_1 = v_1(x_1, t)$
Rys. 7. Wykres $v_1 = v_1(x_1, t)$

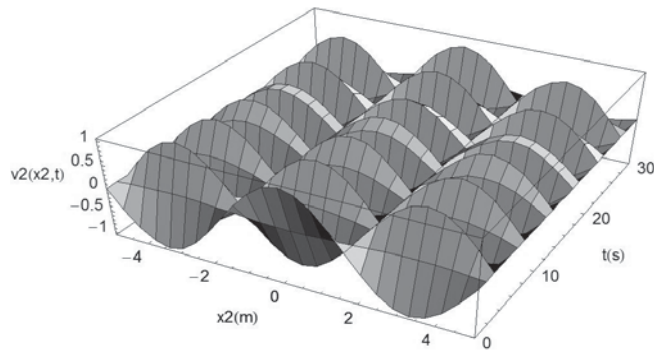


Fig. 8. Graph of $v_2 = v_2(x_2, t)$
Rys. 8. Wykres $v_2 = v_2(x_2, t)$

Graphs of the displacement $w_1(x_1, t) = u_1(x_1, t) + h(x_1)v_1(x_1, t)$ and $w_2(x_2, t) = u_2(x_2, t) + h(x_1)v_2(x_2, t)$ are illustrated on Figures 9, 10.

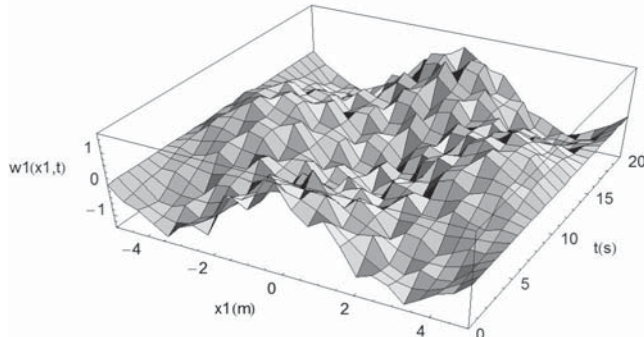


Fig. 9. Graph of $w_1(x_1, t) = u_1(x_1, t) + h(x_1)v_1(x_1, t)$
Rys. 9. Wykres $w_1(x_1, t) = u_1(x_1, t) + h(x_1)v_1(x_1, t)$

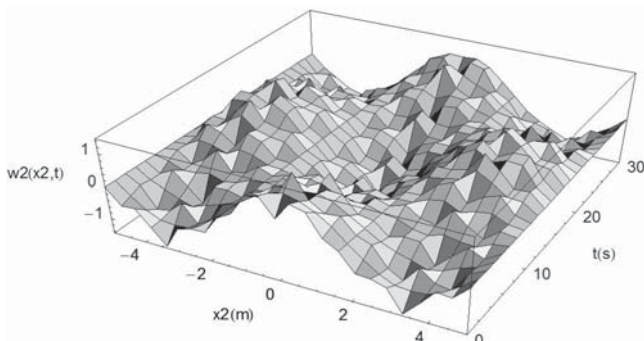


Fig. 10. Graph of $w_2(x_2, t) = u_2(x_2, t) + h(x_1)v_2(x_2, t)$
Rys. 10. Wykres $w_2(x_2, t) = u_2(x_2, t) + h(x_1)v_2(x_2, t)$

Cross-section through the graph of $w_1 = w_1(x_1, t)$ and $w_2 = w_2(x_2, t)$ for the fixed time $t = 15$ s, for the free frequency $n = 1, 2, 5$ is presented on Figures 11, 12.

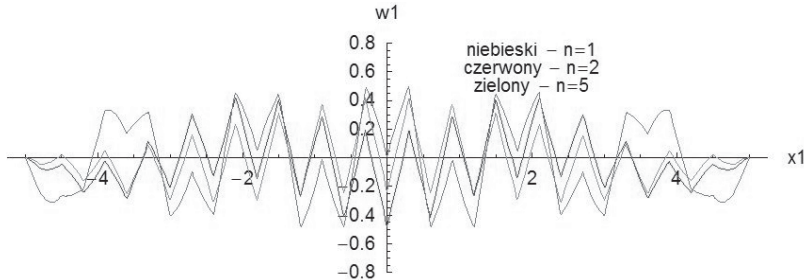


Fig. 11. Cross-section through the graph $w_1 = w_1(x_1, t)$ for the fixed time $t = 15$ s, for various free frequency (n)

Rys. 11. Przekrój przez wykres $w_1 = w_1(x_1, t)$ dla ustalonego czasu $t = 15$ s, przy założeniu różnych częstości drgań własnych (n)

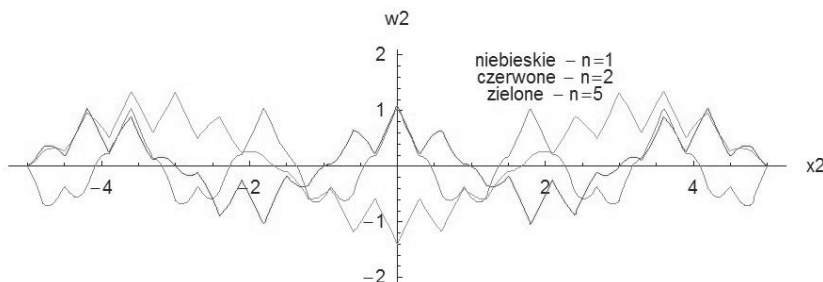


Fig. 12. Cross-section through the graph $w_2 = w_2(x_2, t)$ for the fixed time $t = 15$ s, for various free frequency (n)

Rys. 12. Przekrój przez wykres $w_2 = w_2(x_2, t)$, dla ustalonego czasu $t = 15$ s, przy założeniu różnych częstości drgań własnych (n)

CONCLUSIONS

The above considerations show that the tolerance averaging approach constitutes an appropriate analytical tool for analysis of the dynamic problems of elastic plates reinforced by periodically placed ribs.

REFERENCES

- Nagórko W., Woźniak Cz., 2002. Nonasymptotic modelling of thin plates reinforced by a system of stiffeners. EJPAU 5(2), 1 (www.ejpau.media.pl).
- Thermomechanics of microheterogeneous solids and structures. Tolerance averaging approach, 2008. Eds. Cz. Woźniak et al. Wydaw. Politechniki Łódzkiej, Łódź.
- Woźniak Cz., Wierzbicki E., 2000. Averaging techniques in thermomechanics of composite solids. Tolerance averaging versus homogenization. Wydaw. Politechniki Częstochowskiej, Częstochowa.

DRGANIA WŁASNE W PERIODYCZNIE ZBROJONYCH PŁYTACH SPREŻYSTYCH

Streszczenie. W pracy rozważa się płyty wzmocnione żebrami. Zakładając periodyczne rozmieszczenie żeber w płycie, konstruuje się model uśredniony. Metoda, jaką tu zastosowano, nie jest metodą asymptyczną. W równaniach modelujących pozostaje parametr mikrostruktury (wymiar komórki periodyczności). W celu przetestowania modelu analizuje się przypadek drgań własnych.

Slowa kluczowe: płyta zbrojona, sprężystość płyty, metody homogenizacji, drgania płyt

Accepted for print – Zaakceptowano do druku: 7.07.2010